International Journal of Development Mathematics Vol 1 Issue 4 Page No. 061 - 073

INTERNATIONAL JOURNAL OF DEVELOPMENT MATHEMATICS

ISSN: 3026-8656 (Print) | 3026-8699 (Online)

journal homepage: https://ijdm.org.ng/index.php/Journals

Numerical Solutions for Radiative MHD Casson Nanofluid Flow with Slip, Heat Source, and Chemical Reactions over a Stretching Surface

Aroloye S. Joseph[a*], Fenuga O. John[a] and Abiala I. Olutunji[a]

[a]*Department of Mathematics, Faculty of Science, University of Lagos, Nigeria*

ARTICLE INFO

Article history:
Received 17 August 2024
Received in revised form 05 October 2024
Accepted 19 October 2024

Keywords:
Casson, Viscous dissipation, nanofluid, Slip and Magnetohydrodynamic(MHD).

MSC 2020 Subject classification:
58D30, 82D80, 4K28

ABSTRACT

MHD Casson nanofluid flow in the presence of viscous dissipation, thermal radiation and chemical reaction past a linear stretching surface is investigated. The problem is subjected to slip boundary conditions. The analysis of heat and mass transfer in the presence of Brownian motion and the thermophoretic diffusion effects are incorporated into heat and mass transfer. Nonlinear partial differential equations model governing the problems are transformed into the dimensionless nonlinear ordinary differential equations via similarity variables, then shooting method with sixth-order Runge- Kutta numerical scheme is used to solve the reduce system of Ordinary Differential Equations (ODE). Maple software is used to perform the simulation. The results are presented graphically and in tabular form and the conclusion is drawn that the flow field and other quantities of physical interest are significantly influenced by these parameters. Comparison between the obtained results and previous works are well in agreement. Numerical values of the local skin-friction, Nusselt number and nanoparticle Sherwood number are computed and analyzed. It is noted that the skin-friction coefficient decreases for the larger values of velocity ratio parameter, slip parameter, and increases with an increasing value of Casson parameter. It is also found that enhancing the chemical reaction parameter leads to decrease in concentration profile.

1. Introduction

In the last few years, the non-Newtonian fluids attracted the attention of the mathematicians, physicist, engineers, etc., due to their demanding applications of domestic and industrial usage. In our daily life such applications are all around us, from a morning coffee to an evening bath. Such applications include toothpaste, paints, gels, lubrication oils, polymers, etc., The Navier Stokes equations due to their composite structure, cannot effectively describe the flow of non-Newtonian fluids. In the non-Newtonian fluids, the constitutive equations much more complex than the Navier-Stokes equations. There is no one constitutive equation that can be used to study all non-Newtonian fluids, explaining the complex behaviour of fluids. Jamil and Fetecau (2010) and Rashidi (2016) conducted comprehensive research on non-Newtonian fluids. Elgend *et al.,* (2024) investigated computational analysis of the dissipative Casson fluid flow originating from a slippery sheet in Porous Media. Vishwanath *et al*., (2024) examined the stability analysis of magnetohydrodynamic Casson fluid flow and heat transfer past an exponentially shrinking surface by spectral approach

Casson fluid is categorised under the class of non-Newtonian fluids. Shortcomings of the Bingham fluid model are countered by this model as it explains the nonlinear behaviour seen once the yield stress is achieved. The Casson fluid model successfully explains the physical behaviour of many fluids used in science, engineering and industry. For instance, in chocolate manufacturing industry, the quality of chocolate products depend on the viscosity of the chocolate. Chocolate shows a shear thinning behaviour which is explained best by the Casson fluid model as explained by Goncalves and Lannes (2016). Narender *et al.* (2020) studied the impact of the radiation effects in the presence of heat generation/absorption and magnetic field on the magnetohydrodynamics (MHD) stagnation point flow over a radially stretching sheet using a Casson nanofluid. The method employed by the authors is the shooting method with Adams – Moulton method. Narender *et al.* (2021) investigated the impacts of external magnetic field inclinations and viscous dissipation due to heat generation or absorption parameter on MHD mixed convective flow of Casson nanofluid. They found that with an increase in Casson parameter, the velocity field is suppressing, in parallel with an increase in Casson parameter temperature raised. Govardhan *et al.* (2019) investigated heat transfer with MHD Casson fluid flow towards a linear stretching sheet with temperature distribution over the sheet. They found out that solution depends on Brownian motion number, thermophoresis number, and Prandtl number. Other studies on heat transfer and nanofluid flows are presented in

* Corresponding author. Tel.: +2348073547811
E-mail address: saroloye@unilag.edu.ng (Aroloye S. Joseph.)
https://doi.org/10.62054/ijdm/0104.05

Elelamy, *et al*. (2020), Yousif *et al*. (2019) and Zeeshan, *et al*. (2023) conducted a nanofluid in a stretching sheet in which MHD flow is investigated. The problem was solved by a numerical technique.

Besides, the study of magnetohydrodynamic flow has gained the attention of modern era scientists on account of its extensive industrial and engineering application. Such applications incorporate the design of cooling frameworks by including liquid metals, MHD generators, petroleum industries, accelerators, nuclear reactors, energy stockpiling, pumps, gas turbines and flow meters. Having such an idea as a top priority the scientists and mathematician investigated the behavior of MHD flows in different physical angles. Sheikholeslami *et al*., (2014) studied the properties of magnetohydrodynamic nanofluid. The method employed by the authors is the lattice Boltzmann method. The MHD flow of nanofluid provoked by a stretching surface was examined by Rashidi *et al*. (2014). They found that magnetic fields lead to decrease the nanofluid velocity and increase the nanofluid temperature. Zeeshan *et al*. (2015) investigated the results of magnetic dipole on ferrofluid. They discussed the problem physically for various flow problems. Hayat *et al*. (2015) inspected the consequences of Jeffrey fluid model with convective boundaries. Narender *et al*., (2021) examined the viscous dissipation and thermal radiation effects on the MHD mixed convection stagnation point flow of Maxwell nanofluid over a stretching surface. In this area, various studies have been performed, Ellahi (2013) and Majeed *et al*., (2018)

Thermal radiation is conducted through electromagnetic waves. The energy is transferred due to temperature difference between the two surfaces, and in this process, the energy is spread in the form of waves in all directions. The emission of these radiations depends on temperature surface, nature of surface and frequency of radiations. If the temperature difference is small then linear thermal radiation is applicable, however if the difference of temperature is large then linear thermal radiation is not applicable. In recent years, many researchers focused on the utilization of magnetohydrodynamics along with the thermal radiation phenomenon to study the heat and mass transfer analysis due to its diversified applications. Shah *et al*., (2016) presented numerical analysis of Cattaneo-Christov heat flux model for MHD flow of Maxwell fluid with thermal radiation. The thermal characterization of two-dimensional Maxwell nanofluid flow over a permeable stretching sheet using the finite element method was investigated by Madhu *et al*., (2017). Thermal radiation influences in various fluids with the imposition of different conditions is studied by Endalew and Nayak (2018).

The chemical reaction stimulus play a significant role in the investigations involving heat and mass in areas of science and engineering technology. Zhang *et al*. (2015) studied the effects of chemical reaction and thermal radiation on nanofluids of heat transfer through the porous medium. Sarma *et al*. (2022) considered the problem as a boundary layer flow over a stretching sheet with chemical reaction.
A chemical reaction between the conventional liquid and nanoparticles are classified as a homogeneous reaction during a given phase or heterogeneous reaction i.e., surrounded by a boundary of phase. Reaction rate in the first order chemical reaction is directly related to the concentration. Several authors like Batcha and Katkoori (2023), Yazdi *et al*., (2011) and Daniel, (2017) examined the effect of chemical reaction on nanofluids of heat transfer over a stretching sheet.

The novelty of the present study rests upon the following. The study examines nanofluid flow with Casson fluid as the base fluid and suspended nanoparticles. Important mechanisms such as thermophoresis and Brownian motion effect emphasizes the nanoparticle characteristics are incorporated into the concentration model. The models describing the problem mathematically are formulated to the system of nonlinear partial differential equations and converted into system of coupled nonlinear ordinary differential equations via similarity invariants. A numerical solution of the system of ODEs is obtained by employing the shooting method with sixth-order Runge-Kutta method and the obtained numerical results are compared with similar existing result in literature and there is excellent agreement. The objective is to analyses the influence of embedded flow parameters on flow's velocity, temperature and concentration profiles. To the best of the authors' knowledge, this is the first study to investigate a mathematical model of magnethydrodynamics casson nanofluid with numerical simulation

2 Mathematical modelling

Consider the stagnation point flow of MHD Casson fluid over a stretching surface under the impact of slip wall. Magnetic field of strength β_0 is applied perpendicular to the fluid motion. Additionally, the impacts of Brownian motion and thermophoretic diffusion are also considered. Furthermore, the equations of energy and mass transport are known to determine the profiles of heat and concentration, respectively. The x-axis is aligned with the stretching sheet, and the y-axis is normal to the plate, as shown in Figure 1

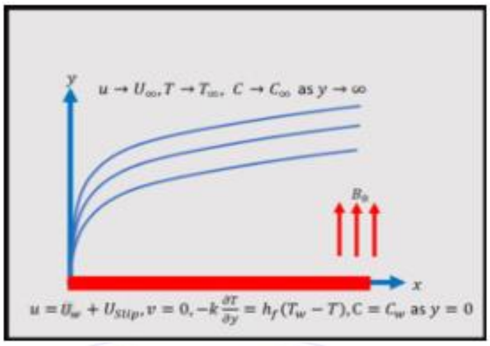

Fig 1. Geometrical view of the Physical mode.

The stretching and slip velocities at the boundary are taken as $U_w(x) = ax$ and $U_{slip} = \left(\mu_B + \frac{P_y}{\sqrt{2\pi_e}}\right)\frac{\partial u}{\partial y}$ respectively, where Py denotes the yield stress, T_w is the surface temperature, μ_B is the plastic dynamic viscosity, π_c represents the critical value of product, $U_\infty = bx, T_\infty, C_\infty$ represent the free stream, velocity, temperature and concentration. Following Swepna *et al*., (2023), the momentum, energy and mass equations model the present problem can be written as

Governing Equations

$$\frac{\partial u}{\partial x} + \frac{\partial u}{\partial y} = 0 \tag{1}$$

$$u\frac{\partial u}{\partial x} + v\frac{\partial v}{\partial y} = v\left(1 + \frac{1}{\gamma}\right)\frac{\partial^2 u}{\partial y^2} + U_\infty\frac{\partial U_\infty}{\partial x} + \frac{\sigma B_0^2}{\rho_f}(U_\infty - u) + \rho_f gB_T(T - T_\infty) + \rho_f gB_C(C - C_\infty) \tag{2}$$

$$u\frac{\partial T}{\partial x} + v\frac{\partial T}{\partial y} = \alpha\frac{\partial^2 T}{\partial y^2} + \Gamma\left\{D_B\frac{\partial C}{\partial y}\frac{\partial T}{\partial y} + \frac{D_T}{T_\infty}\left(\frac{\partial T}{\partial y}\right)^2 - \frac{1}{(\rho C)_f}\frac{\partial q_r}{dy} + \frac{Q_0}{(\rho C_p)}(T - T_\infty) + \frac{v}{C_p}\left(1 + \frac{1}{\gamma}\right)\left(\frac{\partial u}{\partial y}\right)^2\right\} \tag{3}$$

$$u\frac{\partial C}{\partial x} + v\frac{\partial C}{\partial y} = D_B\frac{\partial^2 C}{\partial y^2} + \frac{D_T}{T_\infty}\frac{\partial^2 C}{\partial y^2} - K^*(C - C^*) \tag{4}$$

The related boundary conditions is described as in Ibrahim and Makinde (2015)

Wall conditions $(y = 0)$

$$\left.\begin{array}{l} u = U_w(x) + U_{slip} \Rightarrow u = ax + \left(\mu_B + \frac{P_y}{\sqrt{2\pi_c}}\right) \\ v = 0, -k\frac{\partial T}{\partial y} = h_f(T_f - T), C = C_w \\ \text{Free stream condition}(y \to \infty) \\ u = U_\infty = bx, v = 0, T = T \to T_\infty, C \to C_\infty \end{array}\right\} \tag{5}$$

u and v represent the velocity components in the directions of the x-axis and y-axis, respectively ρ_f is the fluid density, σ denotes the electrical conductivity, T represents the temperature, α is the thermal diffusivity, Γ represents the relation among heat capacity of the antiparticle and the liquid, C is the concentration parameter, μ_B represents the dynamics viscosity, P_y denotes the yield stress, π_c represents the critical value of product and a, b are positive constants. As the heat flux is transported to the body as conduction, the following boundary conditions holds good.

$$k\frac{\partial T}{\partial y} = h_f\left(T_f - T\right)$$

k denotes the thermal conductivity, h_f denotes the coefficient of heat transfer

3 Similarity Transformation

The following developed similarity variables are used to transform Partial Differential Equations (PDEs) to ODEs

$$\left.\begin{aligned} &\eta = y\sqrt{\frac{a}{v}}, \quad \psi = \sqrt{avx}\, f(\eta), \\ &\theta(\eta) = \frac{T - T_\infty}{T_w - T_\infty}, \; \phi(\eta) = \frac{C - C_\infty}{C_w - C_\infty} \end{aligned}\right\} \tag{6}$$

After introducing Equation (6) into Equations (1)–(5),we obtain

$$\left(1 + \frac{1}{\gamma}\right) f'' + ff' - (f')^2 + A + M(A - f') = 0 \tag{7}$$

$$\left(1 + \frac{4}{3R}\right)\theta' + \Pr\left(f\theta' + Ec\left(1 + \frac{1}{\gamma}\right)(f')^2 + Nb\phi'\theta' + Nt(\theta')^2 \right) \tag{8}$$

$$\phi' + Le\Pr\phi' + \frac{Nt}{Nb}\theta' - LeKr\phi = 0 \tag{9}$$

The dimensionless conditions associated with the boundary the boundary are as follows

$$\left.\begin{aligned} &\left.\begin{aligned} &f(\eta) = 0 \\ &f'(\eta) = 1 + \delta\left(1 + \frac{1}{\gamma}\right) f''(\eta) \\ &\theta(\eta) = -Bi(1 - \theta(\eta)) \\ &\phi(0) = 1 \end{aligned}\right\} at \;\; \eta = 0 \\ &\left.\begin{aligned} &f'(\eta) \to A, \; \theta(\eta) \to 0 \\ &\phi(\eta) \to 0 \end{aligned}\right\} \; at \quad \eta \to \infty \end{aligned}\right\} \tag{10}$$

where δ is momentum slip parameter, A is the ratio of stretching velocity of free stream and lower plate. The temperature field depends on the Biot number (Bi) when heat transfer takes place into the fluid

The following expression refers to different parameters used in the above equation

$$\left.\begin{aligned}
&Bi=\frac{h_f}{k}\sqrt{\frac{v}{a}},\ R=\frac{4\sigma^{*}T_\infty^4}{k_0 k},\ M=\frac{\sigma B_0^2(x)}{\rho_f a},\ \ Gr=\frac{B_T g v(T_0-T_\infty)}{U_0^3}\\
&Ec=\frac{u^2}{C_p\left(T_f-T_\infty\right)},\ A=\frac{b}{a},\ \ \Pr=\frac{v}{a},\ \delta=\mu_B\sqrt{\frac{a}{v}}\ ,Gc=\frac{B_c g v(C_0-C_\infty)}{U_0^3}\\
&Nb=\frac{(\rho C)_\rho}{(\rho C)_f v}D_B(C_w-C_\infty),\ L_w=\frac{a}{D_B}\quad Nt=\frac{(\rho C)_\rho}{(\rho C)_f v}D_T(T_w-T_\infty)
\end{aligned}\right\} \tag{11}$$

The physical quantities which govern the flow are the Nusseit (Nu_x), Sherwood number (Sh_x) and skin friction coefficient (C_f) which are given by

$$\left.\begin{aligned}
&Nu_x=\frac{xq_w}{k(T_w-T_\infty)},\quad C_f=\frac{\tau_w}{\rho u_w^2}\\
&\qquad Sh_x=\frac{xh_m}{D_B(C_w-C_\infty)}
\end{aligned}\right\} \tag{12}$$

where heat, mass flux at the surface are q_w and $C_f=-k\left(\frac{\partial T}{\partial y}\right),\ k_w=-D_B\left(\frac{\partial \phi}{\partial y}\right)$ and the skin-friction on flat plate τ_w is given by

$$\tau_w=\left(\mu_B+\frac{p_y}{\sqrt{2\pi}}\right)\left(\frac{\partial u}{\partial y}\right)$$

Using the similarity transformations, we obtain

$$\begin{aligned}
&C_f\ \mathrm{Re}_x^{\frac{1}{2}}=\delta\left(1+\frac{1}{\gamma}\right)f''\\
&\frac{Nu_x}{\sqrt{\mathrm{Re}_x}}=-\theta'(0),\ \frac{Sh_x}{\sqrt{\mathrm{Re}_x}}=-\phi'(0)
\end{aligned} \tag{13}$$

4 Numerical Solution

The system of highly nonlinear differential equations (7), (8) and (9) subjected to boundary conditions (10) is solved by a numerical approach via shooting method with the sixth-order Runge-Kutta method for different moderate values of the flow, heat and mass transfer parameters. The effective Broyden technique is adopted in order to improve the initial guesses and to satisfy the boundary conditions at infinity. Maple software is used for the code and numerical simulation

5 Results and Discussion

This section addresses the numerical solutions in detail, using graphs and tables. This will primarily address the velocity, temperature, and concentration profile. The present results will be compared with those of Hayat *et al*., (2015), Ibrahim and Makinde (2015) and Swepna *et al.,* (2023) for code and simulation verification. The numerical calculations are executed for the observation of the impact of various parametric values of γ, δ, A, Bi, Nb, Nt, Le, Kr on velocity, temperature, mass transfer field.

In Table 1, comparison of Skin Friction Coefficient $-f''(0)$ for different values of δ is displayed. The results were compared with those obtained by Hayat *et al*. (2015), Ibrahim and Makinde. (2015) and Swepna *et al., (2023) and* found both to be in excellent agreement. From table 1, it is observed that skin friction coefficient decreases as slip parameter increases. Table 2 shows the skin-friction coefficient $-f''(0)$ decreases by the increase of A. The effect of δ on Nusselt number $-\theta(0)$ decreases and Sherwood number $-\phi(0)$is opposite as compared to Nusselt number

Table 1: Computational comparison of the values of Skin friction Coefficient $-f''(0)$ with Ibrahim and Makinde (2015) and Swepna *et al.* (2023)

δ	Hayat *et al* (2015)	Ibrahim and Makinde (2015)	Swepna *et al(2023)*	Present Result
0.0	1.000000	1.0000	0 .9999855	0 .9999856
0.1	0.872082	0.8721	0.8720812	0.8720813
0.2	0.776377	0.7764	0.7763964	0.7763966
0.5	0.591195	0.5912	0 .5912748	0 .5912748
2.0	0.283981	0.2840	0 .2841796	0 .2841797
5.0	0.144841	0.1448	0 .1450588	0 .1450588
10.0	0.081249	0.0812	0 .0814330	0 .0814331
20.0	0.043782	0.0438	0 .0439329	0 .0439339
50.0	0.018634	0.0186	0 .0186789	0 .0186789

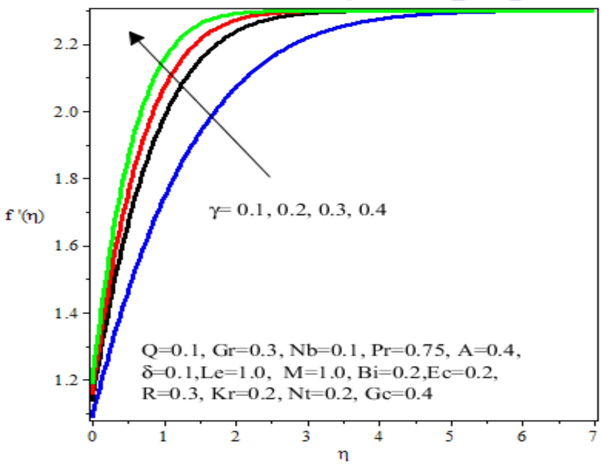

Figure 2. Effect of γ on axial velocity profile

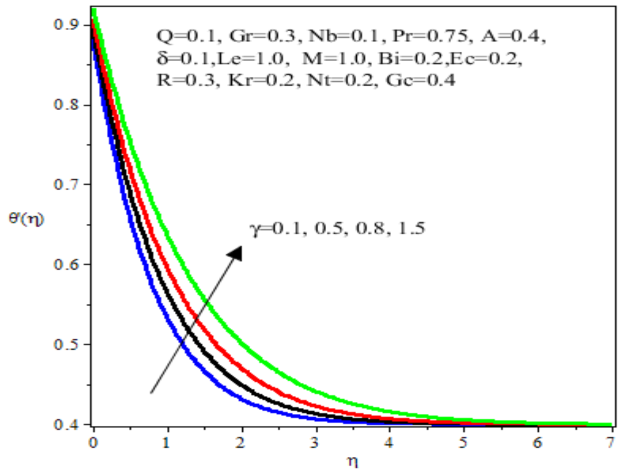

Figure 3: Effect of γ on temperature profile

Figure 2 is drawn to investigate the effect of Casson parameter on the velocity filed. The fluid velocity increases with increasing the value of Casson parameter(γ) . Figure 3 reveals the impact of Casson Parameter γ on temperature distribution. Fluid temperature profile increases as Casson parameter(γ) increases due to the enlargement of surface temperature and thermal boundary layer thickness.

Table 2. Comparison of numerical values of Skin Friction coefficient $-f''(0)$, Local Nusselt number $-\theta'(0)$ and Local Sherwood number $-\phi'(0)$ with Swepna *et al.,* (2023)

			$-f''(0)$		$-\theta'(0)$		$-\phi'(0)$	
A	δ	γ	Swepna *et al.,(2023)*	Present study	Swepna *et al.,(2023)*	Present study	Swepna *et al.,(2023)*	Present study
0.0	0.1		1.1414	1.1414	0.0921	0.0921	2.0434	2.0434
0.1			1.0653	1.0653	0.0923	0.0923	2.0848	2.0848
0.2			0.9791	0.9791	0.0924	0.0924	2.1282	2.1282
0.3			0.8838	0.8838	0.0925	0.0925	2.1730	2.1731
0.9			0.1466	0.1466	0.0933	0.0933	2.4533	2.4533
1.5			-0.8188	-0.8188	0.0940	0.0940	2.7333	2.7333
2.0			1.7622	1.7622	0.0944	0.0944	2.9597	2.9597
2.4			-2.5944	-2.5944	0.0947	0.0947	3.1356	3.1356
0.4	0.2		0.6757	0.6757	0.0924	0.0924	2.1477	2.1477
	0.4		0.5356	0.5356	0.0921	0.0921	2.0464	2.0464
	0.6		0.4449	0.4449	0.0918	0.0918	1.9767	1.9767
	0.8		0.0934	0.0934	0.0916	0.0916	1.9255	1.9255
	0.4	0.1	0.0907	0.0907	0.0915	0.0915	1.9014	1.9014
		0.5	0.2563	0.2563	0.0919	0.0919	2.0018	2.0018
		1	0.3477	0.3477	0.0920	0.0920	2.0245	2.0245

10	0.5356	0.5356	0.0921	0.0921	2.0464	2.0464
100	0.5688	0.5688	0.0921	0.0921	2.0481	2.0481

Figure 4 illustrates the influence of δ on temperature distribution, from the figure it is apparent that especially for cautiously enlarging values of δ, the temperature field is enhanced. Increasing the values of (δ) also raises the sheet surface temperature and the thermal boundary layer depth. Figure 5 indicates the impact of δ on the distribution of dimensionless velocity. It is clearly shown that by an enhancing value of the slip parameter (δ), the velocity profile arises. Generally, the growing values of δ create a frictional resistance between the surface of the sheet and fluid particles escalates, which causes a decrement of the fluid velocity. Figure 6 analyses the effect of free stream velocity (A) on the distribution of dimensionless velocity. From the figure it is apparent that when the free stream velocity is greater than the surface velocity, while the fluid particle velocity accelerates at $A > 1$. Figure7 displays the effect of A on temperature distribution. As the value A heightens, the heat transfer from the sheet to the fluid become smaller and as a result, the temperature falls significantly. Furthermore the thermal boundary layer thickness reduced.

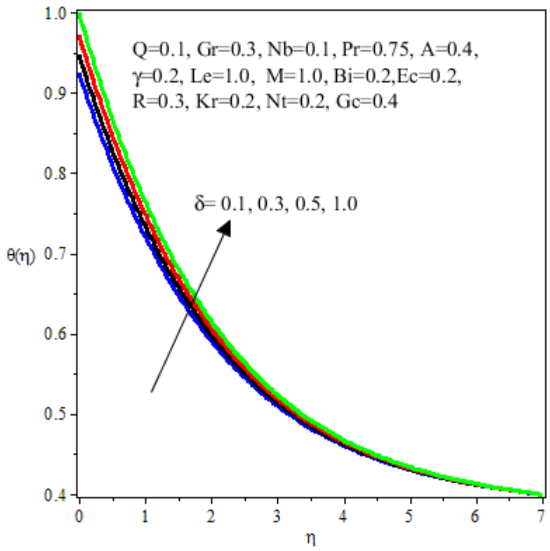

Figure 4. Effect of δ on axial velocity profile

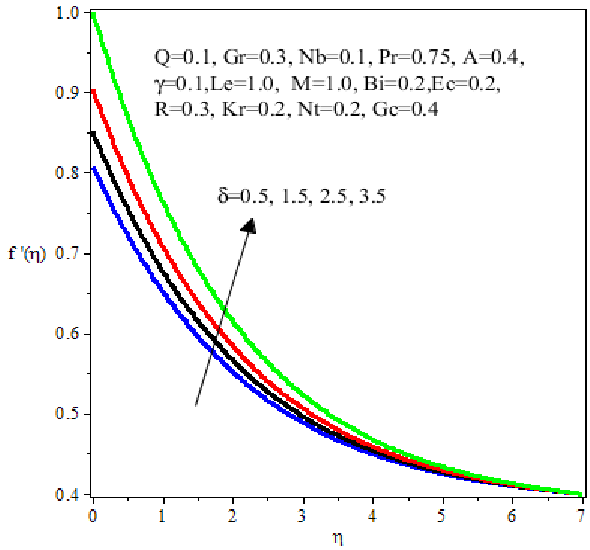

Figure 5. Effect of δ on temperature profile

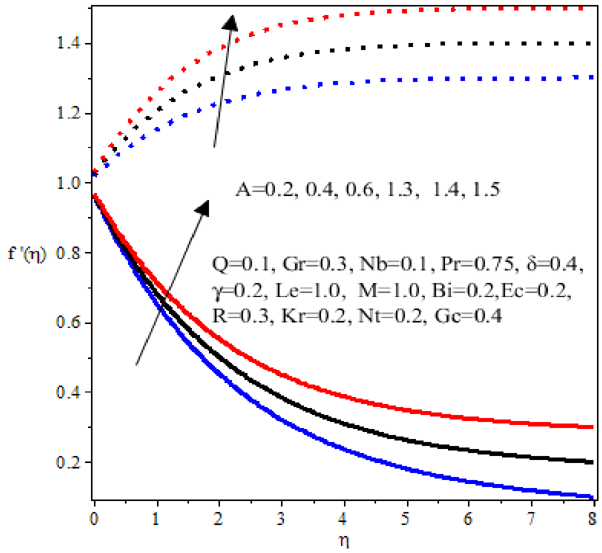

Figure 6. Effect of A on axial velocity profile

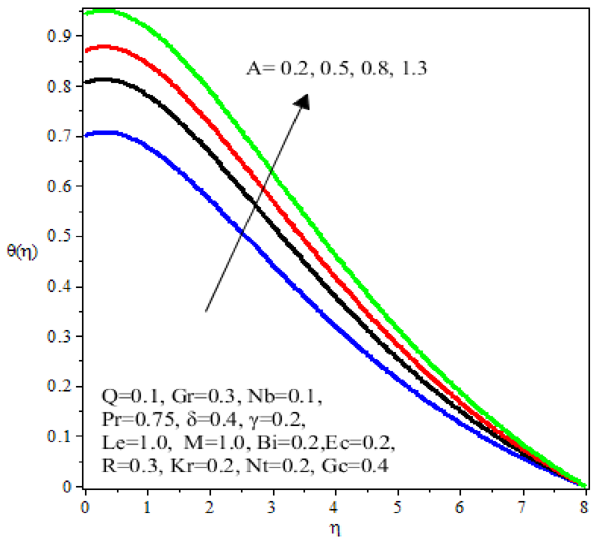

Figure 7. Effect of on temperature profile

Figure 8 reflects the influence of Biot number on the dimensionless temperature distribution. The graph of the velocity profile specifies that an increment in Bi causes an enhancement in the temperature profile. Generally, Biot number is expressed as the ratio of temperature change at the surface to conduction within the surface of the body. As expected, increasing values of Bi enhanced the thermal boundary layer of the fluid.

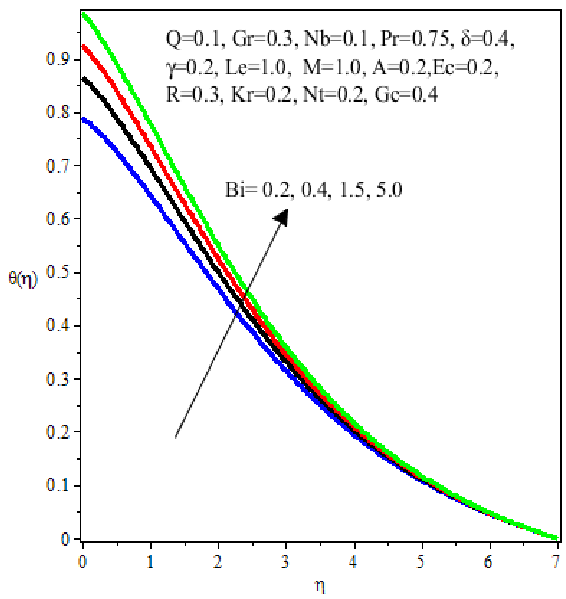

Figure 8. Effect of Bi on temperature profile

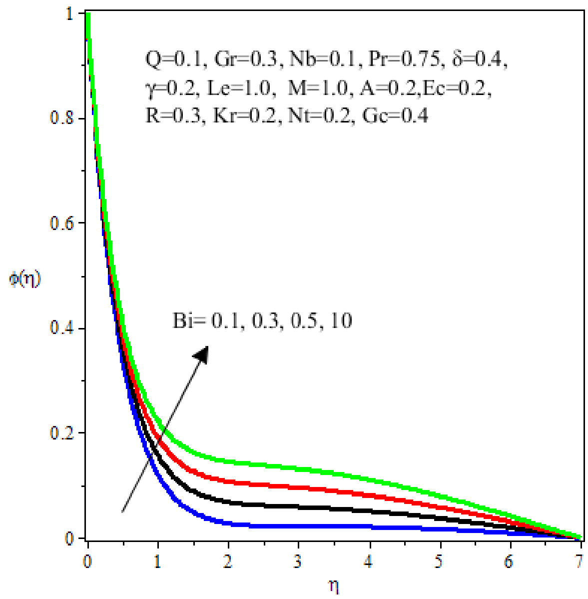

Figure 9. Effect of Bi on concentration profile

Figure 9 depicts the relationship between Bi (Biot number) and the concentration profile. For boosting values of Biot number the graph of dimensionless concentration profile is increased. Increasing Bi means a decrement in the fluid's conductivity because of which the boundary layer of concentration is increased. Figure 10 illustrates the Nt effect on temperature distribution. From the figure it is transparent that the $\theta(\eta)$ field is improved for moderately enlarging values of Nt. In addition, the particles Nt apply a force on the other particles because of which these particles shift from the hotter to cooler regions. Therefore, there is an intensification of the fluid's $\theta(\eta)$ profile. Figure 11 illustrates the impact of Nt on concentration distribution, from the figure for gradually enlarging values of Nt the concentration field is enhanced. Figure 12 analyses the impact of Brownian motion parameter on the temperature distribution. The temperature profile increases marginally for the large values of Nb. This happens due to the reason that as the value of Brownian motion parameter rises, the movement of the nanoparticle enhances significantly which triggers the kinetic energy of the nanoparticles and eventually, the temperature enhances, and thermal boundary layer thickness is magnified.

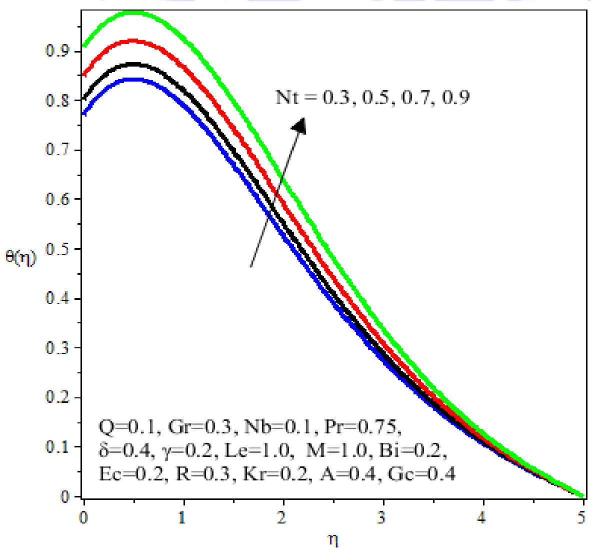

Figure 10. Effect of Nt on temperature profile

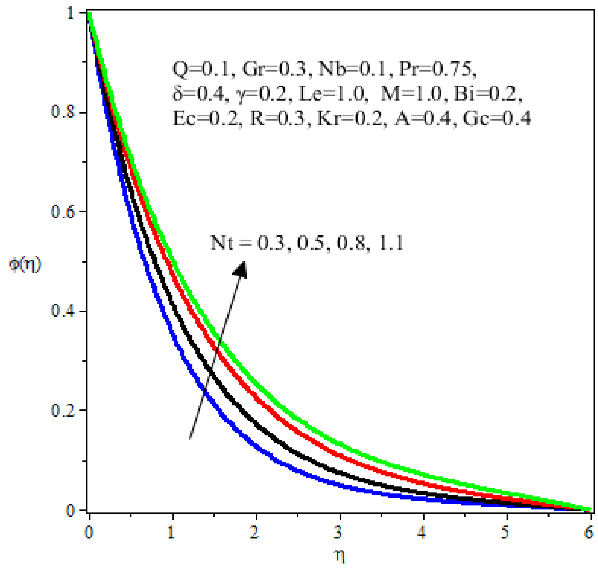

Figure 11. Effect of Nt on concentration profile

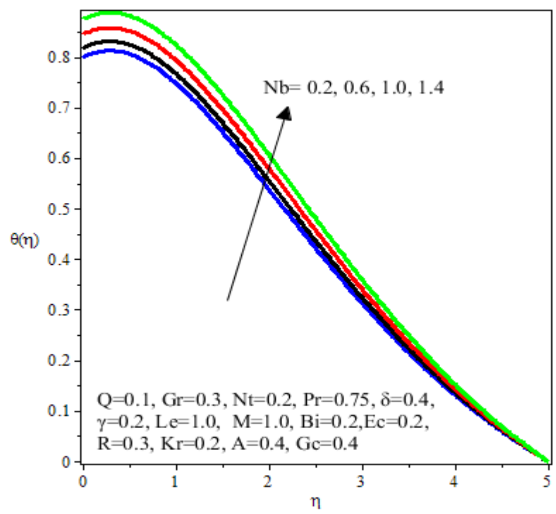

Figure 12. Effect of Nb on temperature profile

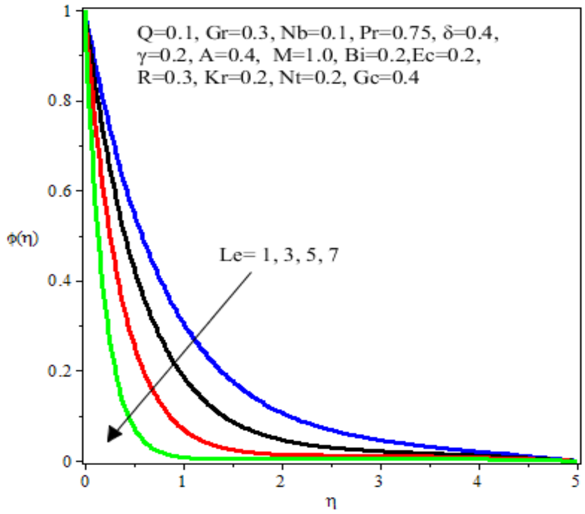

Figure 13. Effect of Le on concentration profile

Figure 13 shows the connection between Lewis numbers and the dimensional concentration distribution. Concentration profile decelerates for the boosting values of Lewis number (Le), physically Lewis number express the respective contribution of rate of thermal diffusion to the rate of species diffusion on the boundary region. As the values of Lewis number (Le) increases leads, fluid concentration decreases. Figure 14 portrays the impact of Eckert number on the temperature field. It is noticed that there is a gradual decrease in the fluid energy by an increment in Ec. Here, it is observed that the temperature increases for gaining the values of Ec. Physically, the Eckert number depicts the relation between the kinetic energy of the fluid particles and the boundary layer enthalpy. The kinetic energy of the fluid particles rises as Ec assume the large values. Hence, the temperature of the fluid climbs marginally and therefore, the associated thermal boundary layer thickness is enhanced.

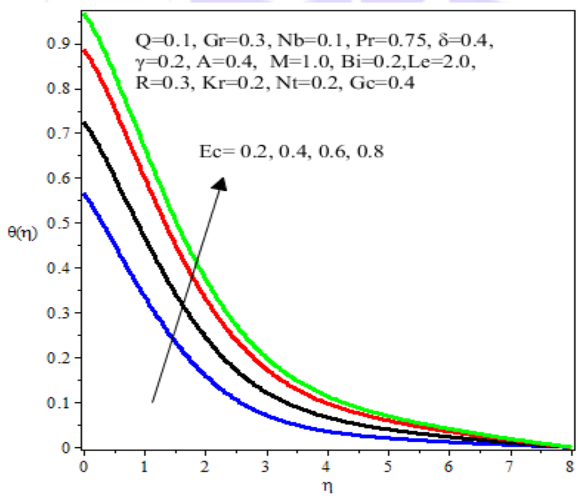

Figure 14. Effect of Ec on temperature profile

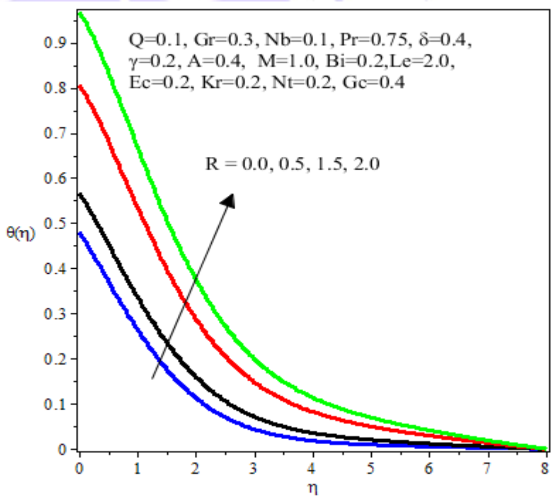

Figure 15. Effect of R on temperature profile

Figure 15 is sketched for the investigation of the temperature profile in response to the thermal radiation parameter R. By increasing the thermal radiation, increase in temperature profile is observed. Physically, a magnification in provides additional heat to the operating fluid which amplifies the temperature field.

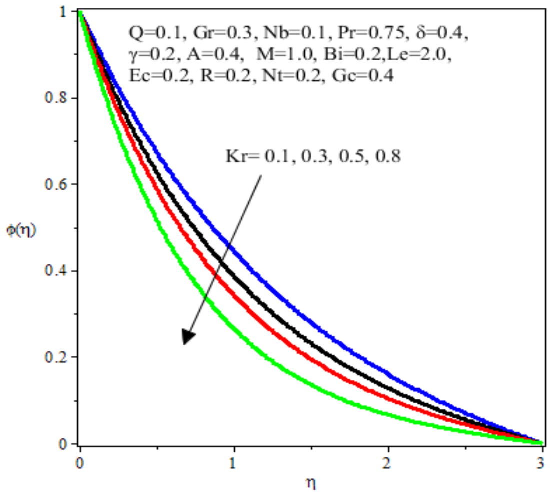

Figure. 16. Effect of Kr on concentration profiles

Figure 16 shows the effects of chemical reaction parameter on the concentration field $\phi(\eta)$. It is noticed that Increasing values of chemical reaction parameter resulted in decrease in concentration. It is because of the fact that the chemical reaction in this system results in chemical dissipation and therefore results in decreases in the profile of concentration. The most significant influence is that chemical reaction tends to decrease the overshoot in the concentration profile and their associated boundary layer.

6 Conclusions

This paper presented numerical simulations of boundary layer flow of MHD Casson nanofluid in the presence of chemical reaction, thermal radiation, heat absorption and chemical reaction. The problem is subjected to slip condition. We transformed the highly nonlinear Partial differential equation governing the problem into a set of ODEs. The numerical solutions are obtained by using the shooting method with Runge-Kutta. Maple is used for the numerical simulations. Our results are excellent agreement with the existing numerical literature results. Different physical parameters are examined and analyzed on fluid flow velocity, temperature and concentrations. In light of the numerical results, the following keynotes are made. The fluid velocity decreases with increasing values of slip and Casson parameters. The fluid temperature increases rapidly as Biot number increases. Brownian motion and thermophoresis parameters increase the fluid temperature profile. Concentration decreases for increasing values of Lewis number and thus lead smaller molecular diffusivity and thermal boundary layer. It is noted that Nu_x is also increased by enhancing the values of Lewis number (Le). Casson parameter rapidly increases fluid concentration and associated boundary thickness. The thermal boundary layer thickness increases for the rise of Eckert number (Ec) as well as radiation parameter (R). Increasing values of chemical reaction (Kr) lead to a reduction in nanoparticle concentration.

Nomenclature

a, b	stretching constant $\left(s^{-1}\right)$
B_0	Magnetic field strength $\left(wbm^{-1}\right)$
D_B	Brownian diffusion coefficient
D_T	Thermophoretic diffusion coefficient
Gr	thermal Grashof number
K	Thermal conductivity $\left(wm^{-1}K^{-1}\right)$
σ^*	Stefan-Boltzmann constant $\left(wm^{-1}K^{-1}\right)$
K^*	Mean absorption coefficient
Ec	Eckert number
Le	Lewis number
M	Magnetic parameter
N_b	Brownian motion parameter
N_t	Thermophoresis parameter
Nu	Nusselt number

Nu_x Reduced Nusselt number
$\Pr$ Prandtl number
P Pressure
C_f Heat capacity of the fluid $\left(Jm^{-3}K^{-1}\right)$
C_p Effective heat capacity of the nanoparticle material $\left(Jm^{-3}K^{-1}\right)$
q_r Radiative heat flux $\left(kgm^{-2}\right)$
q_m Wall mass flux $\left(wm^{-2}\right)$
q_w Wall heat flux $\left(wm^{-2}\right)$
Re_x Local Reynolds number
Shr_x Reduced Sherwood number
T Local Sherwood number
T Fluid temperature (K)
T_w Temperature at the stretching sheet (K)
T_∞ Ambient temperature (K)
u, v Velocity components along x and y axis
u_w Velocity of the stretching sheet $\left(ms^{-1}\right)$
α Thermal diffusivity $\left(m^2s^{-1}\right)$
ϕ Dimensionless nanoparticle volume fraction
η Similarity variable
ψ Stream function $\left(m^2s^{-1}\right)$
θ Dimensionless temperature
ρ_f Fluid density $\left(Kgm^{-3}\right)$
ρ_p Nanoparticle mass density $\left(kgm^{-3}\right)$
σ Electrical conductivity of the fluid
τ Parameter defined by ratio between the effective heat capacity of the nanoparticle material and heat capacity of the fluid.
Gc solutal Grashof number

Reference

Batcha Srisailam, Katkoori Sreeram Reddy, Ganji Narender and Bala Siddhulu Malga, (2023). The Effect of Viscous Dissipation and Chemical reaction on the flow of MHD Nanofluid. *Journal of Advanced Research in Fluid Mechanics and Thermal Sciences*, 107(2), pp. 150-170.

Chaoli Zhang, Liancun Zhang, Xinxin Zhang and Goong Chen., (2015). MHD Flow and radiation heat transfer of nanofluids in porous media with variable surface heat flux and chemical reaction. *Applied Mathematical Modelling*, 39(9), pp. 165 – 181.

Daniel, Y.S., Aziz, Z.A., Ismail, Z., Salah, F., (2017). Entropy analysis in electrical magnetohydrodynamic (MHD) flow of nanofluid with effects of thermal radiation, viscous dissipation and Chemical reaction. 7(4) pp 235-242

Elelamy, A.F., Elgazery, N.S. and Ellahi, R., (2020). Blood flow of MHD non-Newtonian nanofluid with heat transfer and slip effects: Application of bacterial growth in heart valve. *International Journal of Numerical Methods for Heat and Fluid Flow,* 30(11), pp. 4883-4908.

Elgendi, S. G., Abbas, W. Ahmed A. M., Ahmed M. M and Eman, F. (2024). computational analysis of the dissipative Casson fluid flow originating from a slippery sheet in Porous Media. *Journal of Nonlinear Mathematical Physics.*Pp 31:19 https://doi.org/10.1007/s44198-024-00183-3

Ellahi, R. (2013). The effects of MHD and temperature dependent viscosity on the flow of non-Newtonian nanofluid in a pipe: Analytical solutions. *Applied Mathematical Modelling*, 37, pp.1451–1467.

Endalew. M. F. and Nayak, A. (2018). Thermal radiation and inclined magnetic field effects on MHD flow past a linearly accelerated inclined plate in a porous medium with variable temperature. *Heat Transfer-Asian Research*, 48(4),

Gobburu, S. S., Ganji, N. and Kamatam, G. (2022). Radiation effect on the flow of Magneto Hydrodynamic nanofluids over a stretching surface with Chemical reaction, *Journal of Computational Applied Mechanics*, 53(4), pp. 494-509.

Goncalves, E. V. and Lannes, S. C. (2010). Chocolate rheology. *Food Science and Technology*, 30(4), pp. 845-851.

Govardhan K, Narender G, Sarma GS, (2019). Viscous dissipation and chemical reaction effects on MHD Casson nanofluid over a stretching sheet. *Malaysian Journal of Fundamental and Applied Sciences*, 15(4), pp. 585–592.

Hayat, T., Asad, S. Mustafa, M. and Alsaedi, A. (2015). MHD stagnation-point flow of Jeffrey fluid over a convectively heated stretching sheet. *Computers and Fluids*, 108, pp. 179-185.

Ibrahim, W. and Makinde, O. (2015). Magnetohydrodynamic stagnation point flow and heat transfer of Casson nanofluid past a stretching sheet with slip and convective boundary condition. Journal of *Aerospace Engineering*, 04015037. 29(2), pp. 04015037

Jamil, M. and Fetecau, C. (2010). Some exact solutions for rotating flows of a generalized Burgers fluid in cylindrical domains. *Journal of Non-Newtonian Fluid Mechanics,* 165(23-24), pp. 1700-1712.

Madhu, M. Kishan, N. and Chamkha, A. J. (2017). Unsteady flow of a Maxwell nanofluid over a stretching surface in the presence of magnetohydrodynamic and thermal radiation effects. *Propulsion and Power Research*, 6, pp. 31-40,

Majeed A, Zeeshan A, Alamri S.Z, Ellahi R, (2018). Heat transfer analysis in ferromagnetic viscoelastic fluid flow over a stretching sheet with suction. Neural Comput and Applic, 30(6), pp.1979-1955.

Narender, G. Govardhan, K and Sreedhar Sarma, G. (2021). Viscous dissipation and thermal radiation effects on the flow of Maxwell nanofluid over a stretching surface. *Int. J. Nonlinear Anal. Appl*., 12(2), pp. 1267 1287

Narender, G. Govardhan, K. and Sreedhar Sarma, G. (2020). Magnetohydrodynamic stagnation point on a Casson nanofluid flow over a radially stretching sheet. *Beilstein J. Nanotech*nol., 11, pp. 1303–1315.

Narender, G. Govardhan, K. and Sreedhar Sarma, G. (2021). MHD Casson Nanofluid Past a Stretching Sheet with the Effects of Viscous Dissipation, Chemical Reaction and Heat Source/Sink. J. Appl. Comput. Mech., 7(4), pp. 2040–2048.

Rashidi, M. M., Bhatti, M. M. Abbas, M. A. and Ali, M. E (2016). Entropy generation on MHD blood flow of nanofluid due to peristaltic waves. *Entropy*, 18(4), pp. 117.

Rashidi, M., Ganesh, N. V. Hakeem, A. A, and Ganga., B. (2014). Buoyancy effect on MHD flow of nanofluid over a stretching sheet in the presence of thermal radiation. *Journal of Molecular Liquids*, 198, pp. 234- 238.

Shah, S. Hussain, S. and Sagheer, M. (2016). MHD effects and heat transfer for the UCM fluid along with Joule heating and thermal radiation using Cattaneo-Christov heat flux model. *AIP Advances*,

Sheikholeslami, M. Gorji-Bandpy, M. and Ganji., D. (2014). Lattice Boltzmann method for MHD natural convection heat transfer using nanofluid. *Powder Technology,* 254, pp. 82-93.

Swapna, D., Govardhan, K. Narender, G. and Misra, S. (2023). Viscous Dissipation and Chemical Reaction on Radiate MHD Casson Nanofluid Past a Stretching Surface with a Slip Effect, *Journal of Heat and Mass Transfer Research* 10, Serial Number 20, 315 – 328

Vishwanath, B. A, Akash, G., Mahesh, K. N, Gabriella, B. (2024). Stability analysis of magnetohyd-rodynamic Casson fluid flow and heat transfer past an exponentially shrinking surface by spectral approach. *Case studies* *in thermal Engineering. Vol 60. 104810. doi.org/10.1016/j.csite.2024.1048*

Yazdi, M.H. Abdullah, S. Hashim, I. Sopian, K. (2011). Slip MHD liquid flow and heat transfer over non-linear permeable stretching surface with chemical reaction. *International Journal of Heat and Mass Transfer*, 54, pp. 3214–3225.

Yousif, M.A., Ismael, H.F., Abbas, T. and Ellahi, R. (2019). Numerical study of momentum and heat transfer of MHD Carreau nanofluid over exponentially stretched plate with internal heat source/sink and radiation. *Heat Transf. Res.*, 50(7), pp. 649-658.

Zeeshan, A. Majeed, A. and Ellahi, R. (2015). Effect of magnetic dipole on viscous ferro fluid past a stretching surface with thermal radiation. *Journal of Molecular liquids*, 215, pp. 549-554.

Zeeshan, A., Khan, M.I, Ellahi, R., Marin, M., (2023). Computational Intelligence Approach for Optimising MHD Casson Ternary Hybrid Nanofluid over the Shrinking Sheet with the Effects of Radiation. *Appl. Sci*., 13, pp. 95